



## Recent Progress in Copper Based Photocatalysts: (A-Review)

CHANCHAL MONDAL

Department of Chemistry, Mathabhanga College, Mathabhanga, West Bengal-736146, India.

\*Corresponding author E-mail: cmondal15@gmail.com

<http://dx.doi.org/10.13005/ojc/400208>

(Received: December 19, 2023; Accepted: April 03, 2024)

### ABSTRACT

Cu is extremely cheaper and more easily recyclable than Au, Ag. Additionally, Cu nanomaterials induced localized surface plasmon resonance (LSPR) has been found to be tuned from visible to the near infrared spectrum by changing their shape and size and it provides Schottky junction when it is combined with other semiconductor material. It has many other remarkable features. For that reason, Cu based photocatalysis has become a research hotspot in view of its enormous practical applications in dye degradation, catalysis, photocatalytic H<sub>2</sub> production, photocatalytic CO<sub>2</sub> reduction reaction (CO<sub>2</sub>RR) and other topics. Herein, we review the latest advances in copper-based photocatalysts in many fields and their improved activity due to LSPR, Schottky barrier etc. The outstanding characteristics of Cu, principle of LSPR of copper combined with different nanomaterials during photocatalysis are also discussed in detail.

**Keywords:** Plasmon, Photocatalyst, Degradation, Visible light, Mechanism.

### INTRODUCTION

Photocatalysts, due to their potential, are used in water splitting, waste water treatment, dye sensitized solar cell, CO<sub>2</sub>RR and many more. They are used in many areas as they can harvest light energy and convert it to chemical energy.<sup>1,2,3</sup> Among innumerable photocatalysts TiO<sub>2</sub> and ZnO were used comprehensively due to their earth abundance, excellent photostability and non-toxicity.<sup>4</sup> However, semiconductor photocatalysts face few restrictions such as poor light absorption and rapid electron-hole (e<sup>-</sup>/h<sup>+</sup>) recombination. To overcome these shortcomings plasmonic photocatalysis is implemented in a view to enhance the efficiency of the relevant processes. Plasmonic photocatalysts

are capable to exhibit strong optical absorption. This takes place as free surface electrons oscillates on incident of light. The phenomenon is popularly regarded as surface plasmon resonance or SPR. This causes solar energy conversion to increase exponentially. Cu, Au, Ag nanomaterials fetched noteworthy consideration as they are capable to exhibit SPR property to augment photocatalytic action. The striking plasmonic properties make noble metal-semiconductor heteronanoparticles a potential candidate in wide spectrum response photosensitizers. Researchers put a lot of effort into optimizing the morphology, composition, size to improve their performance. Therefore, various metal/semiconductor hybrids, semiconductor heterojunctions have been synthesized and studied.



So far innumerable heterostructures such as Au/TiO<sub>2</sub>, Au/CdSe, Au/ZnO etc have been synthesized and examined for enhancing photocatalytic activity.<sup>5,6,7</sup>

Till date, Au and Ag in various nanostructures with varieties of shape and size are widely exploited as plasmonic photocatalyst. They remained photostable and showed elevated LSPR effect. The plasmonic photocatalytic pathways are explained in detail from the point of view of energy transfer and increased activity of active species. Even though, above two precious noble materials have notable photocatalytic performance, application of them in environmental remediation is limited as they are expensive. Therefore, Cu nanoparticles due to its low cost found to be more beneficial than noble metals in plasmonic catalysis. It is also capable to show excellent LSPR property in wide range of wavelength spectrum. In addition to being highly stable during photocatalysis it has also shown that oxygen molecules (O<sub>2</sub>) as well as water (H<sub>2</sub>O) are competent to oxidize Cu nanomaterials. Again Cu/semiconductor nanocomposite formation is an effective tool for improvement of photocatalytic action. It provides schottky junction in the composite which makes (e<sup>-</sup>/h<sup>+</sup>) separation faster. Cu is also a good conductor. With these advantages Cu-based photocatalysis has progressed steadily in recent years.<sup>8,9,10,11</sup>

A plethora of reviews covering the topic of plasmonic photocatalysis have been published till date. For instances, Liu *et al.*, synthesized hollow Au/Cu<sub>2</sub>O core/shell nanomaterials which exhibited morphology dependent plasmonic band redshifts. Under visible light exposure it is found to be better photocatalyst than Cu<sub>2</sub>O and solid Au/Cu<sub>2</sub>O core/shell nanomaterials.<sup>12</sup> Ag@Cu<sub>2</sub>O core/shell nanomaterials were prepared by Wu *et al.*, which displayed photocatalytic action over a wide range of wavelength owing to its LSPR in the silver core.<sup>13</sup> Mechanism of plasmon-assisted chemical reactions have been reviewed by Scientists. *et al.*,<sup>14</sup> Linic and his colleagues elucidated the mechanism of photocatalysis in different articles.<sup>15,16</sup> At present, ample research efforts have been devoted to non-noble-based catalysis including Cu, In, Ga, Al, Fe, Ni, Co due to their unique ability to slow down the recombination of active carriers and improve rate of photocatalysis.<sup>17,18</sup> Varma *et al.*, in their review article discussed in detail about exploitation

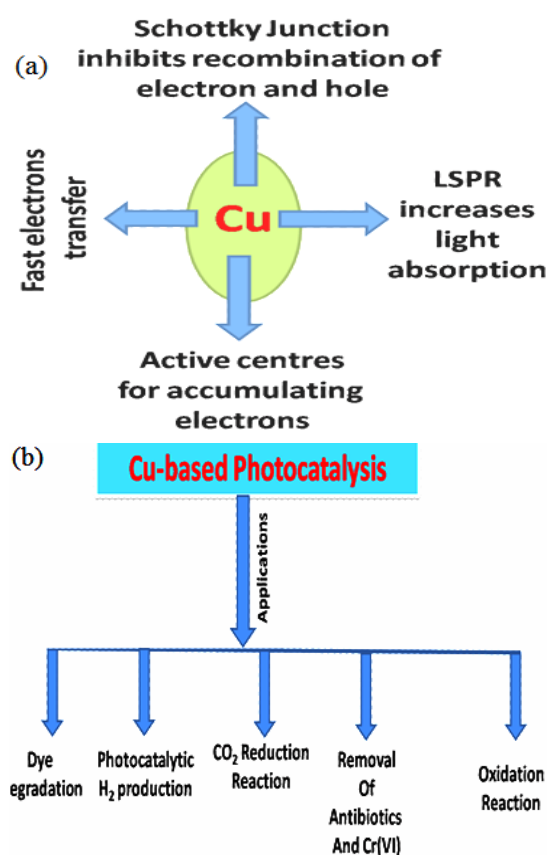
of Cu based nanomaterials in electrocatalysis and photocatalysis.<sup>19</sup> From synthetic developments to potential applications in various fields of Cu related photocatalysis were thoroughly reviewed by Wang *et al.*, They also delved deeply into the challenges, potential outlook for additional improvement of plasmon induced Cu based photocatalysts in their review article.<sup>20</sup>

Herein, we summarize our discussion on exploitation of Cu-based materials in dyes and antibiotics degradation, photocatalytic H<sub>2</sub> evolution, oxidation reaction, removal of antibiotics and CO<sub>2</sub> reduction reaction etc. This review article also introduces the course of action of the plasmonic photocatalysis.

### Various functions of Copper in Photocatalysis

There are few intrinsic properties of copper that can significantly improve photocatalytic properties. Cu induces remarkable enhancement in light absorption capability in the photoactive material and thereby, product selectivity is increased. The unique LSPR property of Cu can harvest NIR light and therefore, broaden its range. When the copper nanoparticle frequency due to the vibration matches with photon frequency under light illumination, photon is absorbed on copper surface. This leads to production of e<sup>-</sup>/h<sup>+</sup> pairs via Landau damping. The active species are separated as the hot electrons are moved to other material connected to copper. The separated electrons and holes can effectively carry out photocatalytic oxidation and reduction reaction, respectively. There are other benefits of copper like it provides lower Fermi level than semiconductor where electrons flow spontaneously. As a result, in Cu/semiconductor nanomaterial, electron flow takes place as long as the Fermi levels have situated in different energy levels. Overall, it decreases semiconductor energy level and forms upward bending energy band barrier. This is known as Schottky barrier and the metal semiconductor junction is known as Schottky junction. This improves separation of active materials and subsequently, their photocatalytic performance. Again, CuO, Cu<sub>2</sub>O, formed due to oxidation of Cu, can also retard e<sup>-</sup>/h<sup>+</sup> recombination. There are other advantages of Cu like it can speed up the electron flow being a good conductor and improves e<sup>-</sup>/h<sup>+</sup> separation. Besides this, Cu nanoparticles are also competent to dissipate heat energy which enhances solar

energy conversion. It is found that widely used  $\text{TiO}_2$ ,  $\text{ZnO}$  are competent to show excellent photocatalytic activity but there are few shortcomings. One of them is there occurs fast recombination of photo-produced electrons and holes. Other one is inadequate light energy absorption. Therefore, the degradation is either slow or not fully achieved. Owing to its above-mentioned manifold advantages copper is combined with nanomaterials such as  $\text{ZnO}$ ,  $\text{TiO}_2$  to obtain superior photocatalytic activity compare to bare nanomaterial.<sup>21,22</sup> Various unique functions of Cu are depicted in Scheme 1a and their applications in different fields are summarized in Scheme 1b.



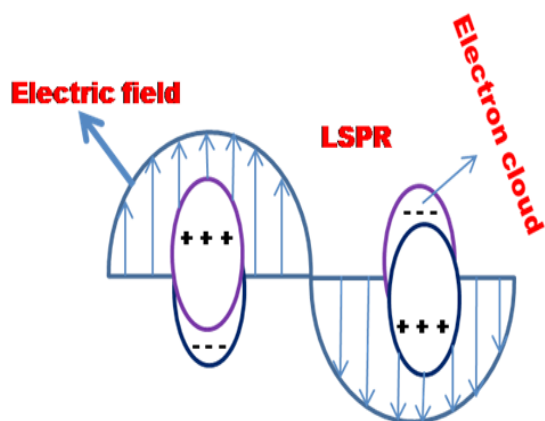
Scheme 1(a). Various functions of Cu; (b) Different applications of Cu-based photocatalysts

### Cu Metal Induced Localized Surface Plasmon Resonance

Noble metal nanoparticles have a special property of extinction in the optical region, often called localized surface plasmon resonance (LSPR). This occurs when photon from a light source hit a nanostructured metal surface (Ag, Au, Cu, Al, doped semiconductors etc.). For LSPR to happen it must meet certain requirements such as the

metals must have high free electron mobility and must be competent to interact with photons. Again, the resonance energy of the oscillating valence electrons on the surface must match with the energy of the photon.<sup>23,24</sup> Resonance energy in Au, Ag, Cu was found to be in the visible energy domain. Collective oscillation of conduction electrons takes place due to interaction among resonant photons and surface electrons causing photon energy to be trapped on the nanomaterial surface for a time greater than the time the photons with light speed spending in that control volume. Due to this effect, photons resonating with plasmon excitation exhibit elevated absorption coefficient as well as capacitive coupling among groups of plasmonic nanoparticles. When an external field is applied, electron cloud is displaced. This results in negative surface charges where electrons are present in excess and positive charges where there is deficiency in electrons. LSPR can produce inhomogeneous electromagnetic (EM) fields, sufficient active species, induces photothermal behaviour, making it an efficient candidate in many fields, e.g., photocatalysis, solar-cells, surface chemistry, chemical reactions, single molecule detection, liquid phase water splitting, hydrogen production and dissociation, photovoltaics and hydrocarbon conversion etc.<sup>25-31</sup> When light incident on plasmonic metals, LSPR concentrates the light energy to its surfaces with elevated EM fields and the strongest EM field intensifies at surface. Field strength decreases with distance from surface. This LSPR excitation in this region causes strong electric field and plentiful energetic electrons at nanostructured surfaces. Thousand fold enhancements in light intensity during resonant photon excitation was seen when isolated cubic shaped Ag nanoparticles were used. Hence, EM field becomes  $10^4$ – $10^6$  times that of incident light along thin junction between two plasmonic nanoparticles. The junctions are called hot spots having very high field strength and are observed to chemisorb and activate reactants for photocatalysis. The photon absorption leads to excitation of electrons, creating  $e^-/h^+$  in plasmonic nanostructured materials. They act as hot charge carriers. The decay of LSPR induces formation of hot electrons resulting in incident photons energy to surpass Fermi energy level. These can carry out necessary photocatalytic chemical changes (Scheme 2).<sup>32-42</sup> The quantum sized metal nanoparticles from 2 to 10 nm are found to exhibit LSPR which can generate hot electrons

with adequate energy and can move to adsorbate for carrying out various activities such as degradation of dye molecules. It is also evident that the LSPR of Ag, Au, Cu nanoparticles varies with their diameters.<sup>43,44</sup>



Scheme 2. Schematic design of LSPR effect in copper nanomaterial. Collective oscillation of conduction electrons caused due to light exposure

## Applications

### Dye Degradation

Dye degradation under UV or visible light exposure is of paramount importance for environmental protection and sustainable development. LSPR plays a crucial role in photo-degradation as light absorption span is increased. Over the past decade, many studies have been conducted on the photo-degradation of innumerable dye molecules exploiting plasmonic Cu-based catalysts. The photocatalytic dye degradation mechanism of  $\text{Cu}_2\text{O}$  and Cu/semiconductor composite is described in the following portions.

CuO is a p-type semiconductor with band-gap of 1.76 eV at room temperature. In its crystal structure it contains oxygen vacancy defects. It is visible light active due to its narrow band-gap.<sup>45</sup> Ramesh *et al.*, utilized CuO as a photocatalyst for degradation many azo dyes such as MB, acid yellow (AY) etc under visible light exposure. When photons (Energy  $\geq$  band-gap energy) hit on CuO nanoparticles, formation of  $e^-/h^+$  takes place. Due to migration of electron to CB there occurs charge separation. These charge carriers, finally, through a series of reactions photodegrade dye molecules.<sup>46</sup> Many researchers also used CuO as a photocatalyst from the past decade.<sup>47,48</sup> In a similar fashion,  $\text{Cu}_2\text{O}$  was also exploited as photocatalyst.  $\text{Cu}_2\text{O}$  is also a

p-type semiconductor with 2.17 eV band-gap and can respond to a wide range of solar light. It is also non-toxic, environmentally benign and inexpensive.<sup>49</sup> Yu *et al.*, employed  $\text{Cu}_2\text{O}$  nanowhiskers to photodegrade p-chloronitrobenzene.<sup>50</sup> Pal *et al.*, employed various morphologies of  $\text{Cu}_2\text{O}$  nanoparticles for visible light photo-degradation of congo red (CR) dye. The facets and surface areas are responsible for various activities of different morphologies. Hollow octahedron and octahedron showed superior activity compare to truncated octahedron, cube and sphere. Hollow octahedron and octahedron are bound by active 111 facets and they have high surface area that makes them better than others. They also showed that 111 facets are more active than 100 facets towards photodegradation.<sup>51</sup> However, due to fast recombination of  $e^-/h^+$  both CuO and  $\text{Cu}_2\text{O}$  suffer limitations in its potential applications as a photocatalyst for dye degradation. To improve photocatalytic activity p/n heterojunction of  $\text{Cu}_2\text{O}/\text{g-C}_3\text{N}_4$  was employed for dye degradation by Zuo *et al.*, Owing to having ample active sites the activity was found to increase.<sup>52</sup> Similarly,  $\text{Cu}_2\text{O}/\text{Cu}_2\text{S}$ ,  $\text{Cu}_2\text{O}/\text{Fe}_2\text{O}_3$  were also explored by researchers.<sup>53,54</sup> CuO was also combined with different materials to remove toxic dye molecules such as  $\text{CuO}/\text{CeO}_2$ ,  $\text{CuO}/\text{Ag}_3\text{PO}_4$  were used for photo-degradation of organic pollutants.<sup>55,56</sup>

Sugawa *et al.*,<sup>57</sup> used a  $\text{Cu}_2\text{O}$ -Cu plasmonic photocatalyst to photodegrade methyl-orange (MO) using visible and near-Infrared-Light exposure. The as-synthesized  $\text{Cu}_2\text{O}$ -CuHS(543) and  $\text{Cu}_2\text{O}$ -CuHS(224) showed 27 and 84 times faster reaction rates than  $\text{Cu}_2\text{O}$ -CuP, respectively. Here 224, 543 represent average diameter in nm scale of silica particles colloid. This huge disparity in photo-activity between the  $\text{Cu}_2\text{O}$ -CuHS arrays and  $\text{Cu}_2\text{O}$ -CuP attributed to the greater surface area of  $\text{Cu}_2\text{O}$ -CuHS arrays and it has almost two times higher activity than planar CuP on its surface. For  $\text{Cu}_2\text{O}$ -CuHS, it was seen to be highest at the respective LSPR wavelength regions indicating the influence of efficient excitation of LSPR of Cu. No intervention of Cu inter-band transition is involved in the degradation of MO. It is also clear that  $\text{Cu}_2\text{O}$ -CuHS(543) showed highest photocatalytic activity due to exposure of NIR light spanning from 700 to 1000 nm.<sup>58,59</sup> Cheng *et al.*,<sup>60</sup> studied the visible-light induced photo-degradation of methylene blue (MB) by  $\text{Cu}_2\text{O}$  microsphere capped with Cu nanoparticles

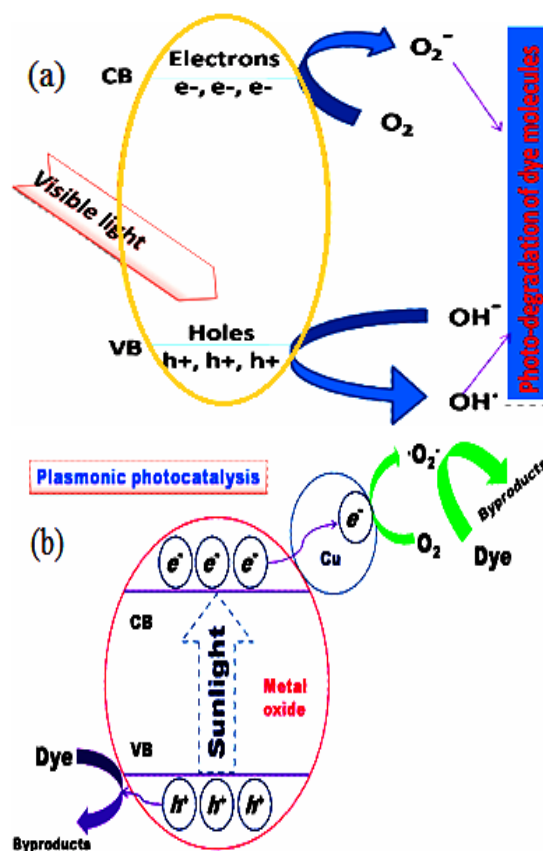
(in nanometer range). The MB photo-degradation was 88% after 60 min of irradiation when Cu<sub>2</sub>O-Cu (S40) (specific mass percentage of Cu in S40 is 10.2%) was employed as a catalyst. This shows that S40 exhibited best photocatalytic activity, which indicates S40 has highest visible-light absorption ability due to the surface plasmon resonance (SPR). The results indicate that exposure of the sample to wavelength below 565 nm does not have significant effect on Cu content of the composite, as SPR of Cu appears at around 565 nm. The improvement was attributed to the effect of SPR on MB that promoted degradation under the irradiation of visible light. Here presence of Cu nanoparticles exploits more visible light absorption due to its SPR effect. This causes more energy transfer to Cu<sub>2</sub>O which enhances active species such as electrons (e<sup>-</sup>) and holes (h<sup>+</sup>) production. Similarly, due to Cu's low work function and excellent conductivity, photo-generated electrons can be smoothly transferred to Cu nanoparticles. In general, recombination of the photo-generated active species was greatly suppressed.<sup>61</sup>

Cu film was also introduced as a broadband absorber which is actually mixture of a lot of absorption peaks. Rekeb and his group.<sup>62</sup> discussed the photocatalytic activity of copper film in Cu<sub>2</sub>O-TiO<sub>2</sub> nanotube arrays (Cu film/Cu<sub>2</sub>O/TiNT). The ternary composite showed excellent photocatalytic performance in the visible spectrum due to presence of copper and cuprous oxide. Their presence in the heterojunction increases significant light absorption as Cu exhibits strong SPR. This leads to electron movement from Cu to Cu<sub>2</sub>O to TiNT and enhances the separation of photo-produced e<sup>-</sup>/h<sup>+</sup> pairs at heterojunction interface. Finally, there occurs excellent improvement in the dye degradation. The Cu film/Cu<sub>2</sub>O/TiNT showed almost three times higher rate of degradation of MB than ordinary TiO<sub>2</sub> nanotube and almost 100% degradation was completed within 30 min after visible light exposure. Pal *et al.*,<sup>63</sup> reported SPR effect of Cu in combination with n-p hetero-junction in ternary nanocomposites for visible light induced MB photo-degradation. They synthesized Cu/Cu<sub>2</sub>O/ZnO which exhibits better photocatalytic action compared to other Cu-ZnO and Cu<sub>2</sub>O-ZnO composite materials. Strong SPR effect of Cu leads to fast movement of photo-generated active species, making the ternary composite a potential visible light driven

photocatalyst. In the ternary nanocomposite, when the materials come into contact, electrons jumped to higher work function (WF) nanomaterial from lower WF nanomaterial. This results in Fermi levels to reach equilibrium. Therefore, Schottky barrier is formed at the metal/semiconductor interface. In the photocatalytic degradation of MB using Cu/Cu<sub>2</sub>O/ZnO photocatalyst, the dye with the nanomaterial is exposed to visible light. At first, due to irradiation there occurs generation of the electrons at the CB and holes at the VB of Cu<sub>2</sub>O (p-type semiconductor). Here ZnO is a n-type semiconductor and a n-p heterojunction is formed between Cu<sub>2</sub>O and ZnO. The CB electrons of Cu<sub>2</sub>O moved to ZnO CB resulting in suppression of recombination of e<sup>-</sup>/h<sup>+</sup>. Again, Cu plays a crucial role in enhancing the photocatalytic activity by producing hot electrons in its CB owing to its SPR effect. The hot electrons produced in the Cu will eventually be transferred to CB of ZnO via different path. This occurs by generating a large number of electrons for photocatalytic degradation of MB. Copper oxide-titanate nanobelt and copper-titanate nanobelt 3D network were exploited to degrade MO by Logar and his team.<sup>64</sup> Photocatalytic activity of the as-synthesized materials in visible light is ascribed to charge transfer from titanate nanobelt to CB of copper and copper oxide. This enhances the lifetime of active species and increases the photo-activity.<sup>65</sup> Zhang *et al.*,<sup>66</sup> utilized Cu-nanoparticle-dispersed amorphous BaTiO<sub>3</sub> for photocatalytic degradation of rhodamine-B (Rh-B). Photocatalytic and photoelectrochemical measurements indicated approximately 3.5 times higher degradation efficiency and 10 times greater photocurrent density of Cu-BaTiO<sub>3</sub> films than the pure BaTiO<sub>3</sub> film (BTO). It also showed high cycling stability. The enhancement in activity is ascribed to both SPR and inter-band excitation effects. Herein, UV-light exposure leads to production of electron (e<sup>-</sup>) in the CB, leaving hole (h<sup>+</sup>) in the VB in BTO. Again, inter-band transition associated SPR effect promotes charge transfer from Cu nanoparticles to BTO. This causes the making of active •O<sub>2</sub><sup>-</sup> radicals on BTO surface for enhanced photocatalytic action. Here, amorphous BTO films serve as h<sup>+</sup> trapping centers which suppress oxidation of Cu to Cu<sup>2+</sup>. The photocatalytic efficiency of CuX/BTO is similar to that of Au/BTO and Ag/BTO counterparts. Wei *et al.*,<sup>67</sup> achieved four times enhancement in photo-degradation rate for MB by dispersing copper nanoparticles on titanium dioxide nanotube arrays.

The sun-light driven superior photocatalytic action of Cu/TiO<sub>2</sub> nanomaterials to pristine TiO<sub>2</sub> is ascribed to Schottky barrier coupled with SPR. This leads to efficient charge separation which makes the photocatalyst a potential material for dye degradation. Enhancement in photocatalytic debromination activities of Cu-TiO<sub>2</sub> on polybrominated pollutants was achieved by Zhao and his co-workers.<sup>68</sup> The as-synthesized Cu-TiO<sub>2</sub> shows fifteen-fold improvement in photocatalytic activity for reductive debromination of decabrominated diphenyl ether (BDE209) than TiO<sub>2</sub>. The significant improvement in photoactivity is because of strong interaction between hydrophobic BDE209 and surface of metal copper. The presence of Cu NPs extends the light absorption range to the visible light region due to SPR. Here oxidation state of Cu remains zero due to reduction of CB electrons of TiO<sub>2</sub> which are produced upon visible light exposure. The copper surface shows catalytic effects by its interaction with BDE209. This leads to activation and subsequent cleavage of C-Br bond. Thus, the rate of reductive debromination of BDE209 is enhanced. Copper nanoparticles placed on silicon nanowire arrays were exploited as an excellent reusable catalyst for degradation of dye molecules, e.g., MB and Rh-B by Zhu and his co-workers.<sup>69</sup> Peng *et al.*,<sup>70</sup> synthesized Cu/ZnO and Cu@CuNi/ZnO hybrid nanomaterials. Both the materials are competent to degrade Rh-B photocatalytically faster than bare ZnO. Herein, the new Fermi energy level of the metal in hetero-nanostructures is placed at lower energy level compare to the CB of pristine ZnO nanomaterials. This results in better photocatalytic action of Cu/ZnO nanocrystals due to decrease in rate of charge recombination and subsequent increased life-time of photo-produced electrons and holes. The maximum photocatalytic action was achieved for Cu/ZnO nanomultipods owing to distinctive morphology of ZnO pods and presence of metal-semiconductor heterointerface that provide better e<sup>-</sup>/h<sup>+</sup> separation and better photocatalytic action. Khiavi *et al.* used CuO/Cu<sub>2</sub>O as a visible light driven photocatalyst for removal of MB. The heterojunction formed between CuO and Cu<sub>2</sub>O played a crucial role to separate charged carriers and thereby, enhance the activity of the material.<sup>71</sup> Cu/Cu<sub>2</sub>O/CuO nanocomposites were used by Kumar *et al.*, for degradation of various dye molecules such as CR and MG. The remarkable increase in activity was attributed to oxygen vacancy in the material

and hetero-junction pattern. The degradation of the composite was found to be better than individual CuO and Cu<sub>2</sub>O.<sup>72</sup> The photocatalytic dye degradation mechanism of Cu<sub>2</sub>O and Cu/semiconductor composite is described in Scheme 3a, 3b; respectively. Table 1 describes Cu-based nanomaterial in photocatalytic dye degradation.



Scheme 3. The photocatalytic dye degradation mechanism of Cu<sub>2</sub>O (scheme 3a) and Cu/semiconductor composite (Scheme 3b)

### Photocatalytic H<sub>2</sub> Production

To achieve significant results in the field of power problems and environmental problems, effective technology with reasonable cost is an attractive way. Photocatalytic H<sub>2</sub> generation is able to meet above-mentioned requirements to provide clean and renewable energy.<sup>73,74</sup>

Hydrogen production through photocatalytic or photoelectrochemical water splitting using solar energy is a notable solution to environmental issues. Starting with the Honda–fujishima effect, a plethora of research has been done to develop effective photocatalysts for H<sub>2</sub> generation.<sup>75,76,77,78</sup> Water

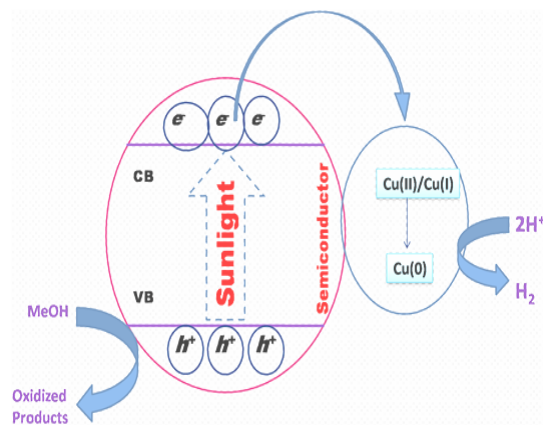
splitting involves Hydrogen-evolution-reaction (HER) and four-electron Oxygen-evolution-reaction (OER). To achieve H<sub>2</sub> generation, Pt, Ir and Ru-based materials are mostly used for HER and for OER but their high-cost, less-abundance, instability severely limit their wide application areas.<sup>79,80</sup> Therefore, finding cheap and functional catalysts is of great importance for researchers. Cu-based catalysts are expected to meet these requirements for photocatalytic H<sub>2</sub> generation as it is cheap and has strong LSPR effect (Scheme 4). Cu-TiO<sub>2</sub> has been employed by many researchers to serve this purpose. For example, Jing *et al.*,<sup>81</sup> used one-dimensional Cu/TiO<sub>2</sub> heterostructures with three to six nm Cu nanoparticles for photocatalytic H<sub>2</sub> generation. Here, the presence of Cu widens significant LSPR absorption range. Here, hydrogen gas is not generated when simulated light having wavelength  $\geq 700$  nm is used. However, amazing result of H<sub>2</sub> production was observed when full spectrum light is illuminated. The improvement is approximately two-fold compared to using UV-Visible light irradiation alone. This means that the photothermal effect caused by SPR plays an important role in promoting photocatalytic activity. Plasmon-induced photothermal effect increases local temperature of catalyst surface. This reduces the activation energy, favouring more effective collisions, which increases reaction rate. This also reduces charge recombination possibility, increases diffusion capability of the reactant molecules and intermediate products.<sup>82,83</sup> These effects are accountable for higher H<sub>2</sub> production. The photothermal conversion during a given photocatalytic water splitting provided new insight for exploitation of full spectrum solar energy. Schneider and his co-workers also employed Cu/TiO<sub>2</sub> for visible light driven photocatalytic H<sub>2</sub> production.<sup>84</sup> Due to incident of visible light on Cu/TiO<sub>2</sub> surface, charge carriers are formed. It can be done by either directly exciting TiO<sub>2</sub> surface or through copper-SPR induced excitation of the metal oxide surface. These methods happened across entire visible light wavelength ( $\geq 420$  nm) but longer wavelengths of light ( $\geq 500$  nm) leads to the photocatalytic action only due to Cu-SPR effect. TiO<sub>2</sub> under exposure of wavelengths above 420 nm is not competent to produce hydrogen. It turns out that copper nanoparticles play an important role in co-catalysts in energy conversion due to its higher light harvesting efficiency at higher wavelengths. Peng *et al.*,<sup>85</sup> also introduced copper nanoparticles-

decorated TiO<sub>2</sub> nanotube array for photocatalytic hydrogen evolution under visible light. The photocatalyst remained stable and showed excellent performance owing to strong SPR of Cu evenly distributed on TiO<sub>2</sub> nanoarrays. This significant activity is attributed to production of electrons and an EM field in the photocatalyst. These hot electrons move towards the CB of TiO<sub>2</sub> and thus got separated from holes. This reduces the chance of recombination of e<sup>-</sup>/h<sup>+</sup> and thus, improving efficiency. Ruediger *et al.*,<sup>86</sup> exploited Cu decorated TiO<sub>2</sub> for hydrogen generation from water under light exposure. However, Cu in the matrix suffers Ostwald's ripening i.e., it is oxidised to copper oxide and forms Cu<sup>2+</sup>, Cu<sup>+</sup> ions in water. This reconstructs the photocatalytic system which retards the catalytic activity. Carbon was added to TiO<sub>2</sub> to prevent Ostwald's ripening through encapsulation of CuOx (Cu/CuO/Cu<sub>2</sub>O) system. Under light irradiation, reduction of CuO takes place, whereas, Ostwald's ripening is prevented. This Operando photoswitching mechanism generates Cu in the material which increases H<sub>2</sub> production activity through SPR. Zeng *et al.*,<sup>87</sup> prepared Cu nanoparticles on CuFe<sub>2</sub>O<sub>4</sub> (cuprospinel) surface. The photocatalytic HER performance of CuFe<sub>2</sub>O<sub>4</sub> is increased due to LSPR of Cu nanoparticles. It contributes to the separation function of photo-generated e<sup>-</sup>/h<sup>+</sup>, which improves activity of the as-prepared materials manifold towards photocatalytic hydrogen evolution. Here, LSPR effect of copper nanoparticles deeply influences utilization of photons which increases its catalytic efficiency. The sample having 1.2% weight of Cu in CuFe<sub>2</sub>O<sub>4</sub> showed highest hydrogen evolution rate (2.26 mmolg<sup>-1</sup>h<sup>-1</sup>) which is almost four times higher than blank CuFe<sub>2</sub>O<sub>4</sub> whose hydrogen evolution rate is 0.45 mmolg<sup>-1</sup>h<sup>-1</sup>. Cu based heterojunction was used as plasmonic photocatalyst for H<sub>2</sub> production by Lou and his group.<sup>88</sup> They employed lollipop-shaped Cu@Cu<sub>2</sub>O/ZnO nanoaterial for photocatalytic H<sub>2</sub> production through water-splitting. The heterojunction exhibits remarkable photcatalytic activity and found to be superior to bare ZnO nanomaterial because of plasmonic copper in the material. The as-synthesized heterojunction with 30 wt% Cu@Cu<sub>2</sub>O exhibited the manifold greater rate in comparison to Cu@Cu<sub>2</sub>O and ZnO. Distinctive design of Cu@Cu<sub>2</sub>O/ZnO heterojunction permits the efficient electronic transfer through the Cu to Cu<sub>2</sub>O to ZnO pathway. This improves photocatalytic H<sub>2</sub> evolution remarkably.



Cu-SrTiO<sub>3</sub> (where Cu size ranges from 2.8 to 7.7 nm) was introduced for H<sub>2</sub> production under visible light exposure by Liu and his co-workers.<sup>89</sup> The as-synthesized nanomaterial showed five times greater H<sub>2</sub> evolution than Cu. The analysis indicates that Fano-interference is decreased between inter-band transition and LSPR with enlargement of copper nanoparticles radius. This enhances the lifetime of photo-produced carriers. The results revealed that the as-synthesized material will become an efficient candidate in the field of water splitting and will decrease reliance on costly Ag, Au for this purpose. Zeng *et al.*,<sup>90</sup> exploited nonsemiconductor plasmonic CuCo bimetal for enhanced solar-driven photocatalytic water splitting. The photocatalyst shows excellent stability even after four consecutive cycles and on sun-light exposure shows outstanding activity towards production of H<sub>2</sub> (77.1 μmol/g<sup>-1</sup>h<sup>-1</sup>). No sacrificial agent was exploited in this reaction. Upon exposure of sun-light on bimetallic surface there occurs generation of e<sup>-</sup>/h<sup>+</sup> pairs by way of Landau Damping.<sup>91,92</sup> Then plasmon driven electrons gathered on Cu surface and were moved to Co due to a superior WF. The electrons act as charge carriers. Co nano-sheets reduce recombination process of e<sup>-</sup>/h<sup>+</sup> pairs. After that, these active carriers on the surface of Co nano-sheets converted the adsorbed water molecules into H<sub>2</sub> while, the neighboring water molecules interacted with photo-generated holes on the Cu to generate O<sub>2</sub>. Another CuCo bimetal was combined with reduced graphene oxide (rGO) by Zhang *et al.*,<sup>93</sup> for plasmon assisted photocatalytic water splitting. It was done without any sacrificial agent. The CuCo bimetal with rGO was competent to convert the solar energy into SPR oscillations and transferred the e<sup>-</sup>/h<sup>+</sup> pair through Landau damping. Electrons present in the bimetal spontaneously moved to rGO. This kind of synergistic interaction efficiently slows down recombination of the e<sup>-</sup>/h<sup>+</sup> pair compared to the bare CuCo bimetal and pure Co. In a similar fashion Zeng and his team<sup>94</sup> exploited dendrite like CuNi/rGO composite which showed improved H<sub>2</sub> evolution rate. Cu was also anchored on metal chalcogenides to obtain surface plasmon assisted hydrogen evolution. Xu *et al.*,<sup>95</sup> employed Cu/WS<sub>2</sub> for photoreduction of H<sub>2</sub>O to H<sub>2</sub>. The optimized WS<sub>2</sub>@Cu hybrid material remained stable and showed amazing H<sub>2</sub>-evolution rate under sun-light exposure. The rate is almost 40 times greater than pure WS<sub>2</sub>. The SPR of Cu nanomaterial makes hot electron

transfer to WS<sub>2</sub> nanomaterial possible. That is why it showed excellent photoactivity. Table 2 describes Cu-based nanomaterial in H<sub>2</sub> production under exposure of light source.



Scheme 4. Schematic illustration of Cu-based photocatalytic H<sub>2</sub> generation

#### Photocatalytic Carbon dioxide Reduction Reaction

Humans as well as other animals are facing harshness due to steady increase of global temperature that results in unwanted climate change. Increase in carbon dioxide concentration in the air is one of the reasons of global warming. Therefore, controlling the CO<sub>2</sub> emissions is top-most priority of the researchers to save mankind from future disaster.<sup>96,97</sup> Carbon dioxide reduction (CO<sub>2</sub>RR) using solar light into precious chemical fuels provides a sustainable and attractive method for future energy rich fuels. Furthermore, it diminished highly hazardous CO<sub>2</sub> discharge to a significant extent. CO, CH<sub>3</sub>OH, CH<sub>4</sub> are the common products of CO<sub>2</sub>RR. It also results in the formation ethylene, ethane, and ethanol. Semiconductors, metal-organic frameworks (MOFs), inorganic perovskite halides are used extensively in CO<sub>2</sub>RR, but reduced catalytic activity and large band-gap, low electron-transfer efficiency prohibit them to become a competent candidate in CO<sub>2</sub>RR.<sup>98,99,100</sup>

CO<sub>2</sub>RR through photocatalysis usually involves three steps which are summarized here. (1) At first, suitable photon absorption occurs by the semiconductor and e<sup>-</sup>/h<sup>+</sup> pairs are produced subsequently. (2) Then the active species migrated towards the surface (3) Finally, CO<sub>2</sub> is reduced by the photo-electrons, whereas, O<sub>2</sub> is produced by the oxidation of water by holes. Adsorption of CO<sub>2</sub> and desorption of the products are crucial for the reduction

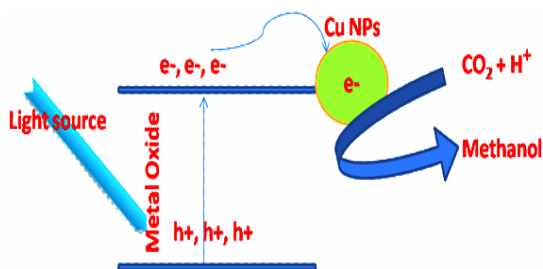


process. Cu, due to its various outstanding properties in combination with other nanomaterial, is competent to reduce CO<sub>2</sub> photocatalytically (Scheme 5).

Cu-loaded TiO<sub>2</sub> porous-material has been introduced by Zhang *et al.*,<sup>101</sup> It exhibited good CO<sub>2</sub>RR activity under solar-stimulated light. Highest CH<sub>4</sub> production output of almost 8.04 μmol/g.h, was attained with 0.4 wt% Cu in the nanomaterial. It was 21 times more than commercially obtained TiO<sub>2</sub>. Here Cu traps electrons and separates them from holes efficiently. The electrons now move to TiO<sub>2</sub> surface and start reducing CO<sub>2</sub>. XPS study and Auger Cu LMM reveal that Cu(0) is present on TiO<sub>2</sub> surface. H<sub>2</sub> production runs parallel when CO<sub>2</sub>RR is going on. This decreases CO<sub>2</sub>RR rate. Cui *et al.*,<sup>102</sup> through solvothermal technique, produced Cu@TiO<sub>2</sub> photocatalyst. In this context, the incorporated Cu in the semiconductor not only improves rate of photocatalysis but also enhances CO<sub>2</sub>RR selectivity by retarding H<sub>2</sub> production. This attributes to fast transfer of electrons from semiconductor to Cu in Cu@TiO<sub>2</sub> photocatalyst. This takes place as the Fermi level of Cu is placed below the semiconductor level. The electron rich Cu serves as active site. In this process, CO production is increased while that of H<sub>2</sub> is decreased due to greater adsorption of CO than H<sup>+</sup> on Cu surface. Jiang *et al.*,<sup>103</sup> synthesized Cu-dispersed TiO<sub>2</sub> ultra-thin nano-sheet. This can substantially forms CO from CO<sub>2</sub> under solar irradiation. The catalyst can be re-cycled for further use. In this process, Cu<sup>2+</sup>, being positively charged, is readily adsorbed on the negative TiO<sub>2</sub> surface. Upon exposure of solar light the photo-produced electrons reduce Cu<sup>2+</sup> to metallic Cu(0). The process is favored in CO<sub>2</sub> atmosphere as presence of oxygen leads to further oxidation of Cu(0) to Cu<sup>2+</sup> in aqueous system. The electrons on Cu(0) on reaction with CO<sub>2</sub> forms CO and O<sub>2</sub><sup>-</sup> ion through HCO<sub>3</sub><sup>-</sup> and CO<sub>3</sub><sup>2-</sup>. On the other hand, holes present in the VB of TiO<sub>2</sub> produces O<sub>2</sub> and H<sup>+</sup> by oxidising water. The proton reacts with oxide ion and completes the cyclic process. Yuan *et al.*,<sup>104</sup> synthesized atomically dispersed Cu species on meso-porous TiO<sub>2</sub> (m-TiO<sub>2</sub>) for carrying out CO<sub>2</sub>RR photocatalytically. Cu dispersion causes facile multi-electron reduction which leads to huge enhancement in CO<sub>2</sub>RR activity. In this mechanism, initially adsorption of CO<sub>2</sub>, H<sub>2</sub>O occurs on mesoporous TiO<sub>2</sub> through diffusion of the adsorbates. After that, photo-produced e<sup>-</sup>/h<sup>+</sup> pairs which are trapped by

Cu and surface hydroxyl groups, respectively. This boosts their separation. The Cu(II) present initially reduced to Cu(I) and then to Cu(0) by electrons. Again, the trapped holes could oxidize Cu(0) back to Cu(I) and Cu(II). Therefore, the Cu-species can attack electrons more. As a matter of fact, the Cu species could attack electrons more proficiently to carry out reduction faster than the oxidation. This results in formation of Cu(0) from other Cu-species and photocatalyze CO<sub>2</sub>RR. While, holes activate adsorbed H<sub>2</sub>O and hydroxyl groups on the m-TiO<sub>2</sub> surface to produce O<sub>2</sub> and H<sup>+</sup>. In this regard, the Cu-species are competent to capture photo-generated electrons to support the multi-electron CO<sub>2</sub>RR to CH<sub>4</sub>. Fan *et al.*,<sup>105</sup> exploited Cu/TiO<sub>2</sub> nanoflower to reduce carbon dioxide to CH<sub>3</sub>OH. This Cu/TiO<sub>2</sub> film was found to show superior photocatalytic action for the CO<sub>2</sub>RR. With 0.5 Cu/TiO<sub>2</sub> nanoflower, under UV-Vis light illumination, CH<sub>3</sub>OH production rate was seen six-fold faster rate compare to bare TiO<sub>2</sub> film. The increase of activity corroborates with SPR of Cu nanoparticles. First, irradiation creates electrons in CB of TiO<sub>2</sub> with subsequent transfer to Cu cluster. Afterwards, due to the LSPR effect electrons become more energetic. This leads to facile reaction of electrons with CO<sub>2</sub> species. The energetic VB holes in TiO<sub>2</sub> oxidize H<sub>2</sub>O or OH<sup>-</sup> to form OH., which produce oxygen and hydrogen ion. Hydrogen ion and active electron accelerate the formation of CH<sub>3</sub>OH through reducing CO<sub>2</sub>. Similarly, SPR effect of Cu is exploited for improved photo-reduction of CO<sub>2</sub> into CH<sub>3</sub>OH by Ye *et al.*,<sup>106</sup> They utilized Cu/ZnO photocatalyst for this purpose. Cu/Co core/shell bimetal was introduced by Song and his team<sup>107</sup> for selective photocatalytic CO<sub>2</sub> reduction. The as-synthesized material showed outstanding activity reducing carbon dioxide to carbon monoxide with high CO production rate. Herein, no photo-sensitizer and co-catalyst were used. In addition to this the Cu/Co exhibited excellent CO selectivity and remained stable for 48 hours. This enhancement is attributed to plasmon-induced carrier separation by the as-prepared materials. The LSPR effect in metals via Landau damping generates charge carriers to take part in the selective reduction. This suitable WF of the bimetal boosts movement of the active species upon light illumination and thereby increases the photo-reduction. Cu was also incorporated into other materials such as CeO<sub>2</sub> by Wang *et al.*,<sup>108</sup> This was done in a view to enhance

the oxygen vacancy. This leads to huge alteration of band-gap and electronic conductivities. This makes the photocatalyst to harvest more light, increase  $e^-/h^+$  separation efficiency. Therefore, there occurs more absorption and subsequent activation of  $\text{CO}_2$  which ultimately, results in increase in photocatalytic action. Hu *et al.*,<sup>109</sup> photodeposited Cu on  $\text{Bi}_4\text{O}_5\text{I}_2$  micron-flower for photocatalytic  $\text{CO}_2\text{RR}$ . There are two severe flaws in photocatalysis by  $\text{Bi}_4\text{O}_5\text{I}_2$ . One of them is its poor light harvesting capability and other one is speedy recombination of photo-produced carriers. That's why the photocatalysis gives poor outputs. However, combination of Cu with the material generates few advantages. One is SPR due to presence of Cu and other is formation  $\text{Cu}/\text{Bi}_4\text{O}_5\text{I}_2$  Schottky junction. SPR effect, due to visible light irradiation, produces hot electrons which migrate to CB of  $\text{Bi}_4\text{O}_5\text{I}_2$  micron-flower. These carry out the  $\text{CO}_2\text{RR}$ . Again, electrons back-flow is effectively prevented by Schottky barrier so that the holes carry out the  $\text{H}_2\text{O}$  oxidation. Kuang *et al.*,<sup>110</sup> exploited  $\text{Cu}/\text{CsCuCl}_3$  nano-heterojunction for photo-reduction of  $\text{CO}_2$  to  $\text{CH}_4$ . The presence of  $\text{Cu}(0)$  boosts charge separation, promotes  $\text{CO}_2$  activation, provides stabilization to the intermediates. It provides almost three times more electron consumption than bare  $\text{CsCuCl}_3$ . Selectivity for methane production is also increased in the heterojunction than the bare material. Table 3 describes Cu-based nanomaterial in photocatalytic  $\text{CO}_2\text{RR}$ .



Scheme 5. Schematic depiction of Cu-based photocatalytic  $\text{CO}_2\text{RR}$

### Oxidation Reaction

The oxidations of organic compounds have a solid impact in energy conversion and pollution mitigation. However, high activation energy of  $\text{O}_2$  during usual reaction is not good for catalyst stability and selectivity of product. Inexpensive Cu-based materials can be good catalysts for  $\text{O}_2$  dissociation through hot electrons.

Linic and his co-workers<sup>111</sup> described

catalytic epoxidation of propylene to form propylene oxide on copper nanoparticles photothermally. There occurs significant selective steady state enhancement upon exposure of the catalyst in visible light. Photoexcitation of the LSPR of Cu decreases surface Cu atoms upon visible-light illumination. Therefore, rate of reaction is improved. Zhu and coworkers<sup>112</sup> utilized Cu nanoparticles supported on titanium nitride for visible-light induced epoxidation of alkenes. Significant electron transfer between Cu NPs and titanium nitride indicates the retention of Cu NPs in metallic states that activate  $\text{O}_2$  molecule and increases adsorption of alkenes chemically. The photocatalyst showed excellent reusability and stability. Wavelength and intensity of light also found to influence the reaction process.

### Photocatalytic Degradation of Antibiotics

Removal of antibiotics has aroused a great deal of consideration due to its severe impact on marine systems and other creatures.<sup>113</sup>  $\text{Cu}@\text{TiO}_2$  was exploited by Gan and his team to remove ciprofloxacin (CPFX) through photodegradation. Very small Cu content (0.1 wt%) in the hybrid found to display excellent photocatalytic activity. Three-fold enhancement in photocatalytic action was observed with 0.1wt% Cu hybrid owing to greater separation efficiency of photo-produced electrons and holes during photocatalysis.<sup>113</sup> In a similar way,  $\text{Cu}/\text{Ag}_3\text{PO}_4$  nanomaterial was employed to degrade CPFX by Liu *et al.*,<sup>114</sup>

### Photocatalytic Removal of Cr(VI)

Cr in its +6 oxidation state is highly lethal for human beings and marine creatures. However, in its +3 oxidation state it becomes highly necessary for living organisms. Therefore, reducing Cr(VI) to Cr(III) is a burning issue for the researchers. Photocatalysis is a unique technique to remove Cr(VI) due to its less hazardous and less costly approach.<sup>115</sup> Patnaik *et al.*, incorporated copper inside  $\text{MoO}_3/\text{g-C}_3\text{N}_4$  nanocomposite. Herein,  $\text{MoO}_3$  and  $\text{g-C}_3\text{N}_4$  form a z-type heterojunction that can effectively reduce a toxic pollutant Cr(VI). Introducing Cu in the composite leads to enhancement in photocatalytic activity and almost 95% reduction of Cr(VI) was achieved. Double Z-scheme charge transfer along with oxygen deficiency in  $\text{MoO}_3$  is the reason for enhancement in photocatalytic activity. LSPR of Cu helps absorb more visible light and converts more number of photons to electrons. As a result, CB of  $\text{CuO}$  has sufficient electrons to carry out the reduction reaction.<sup>116</sup>

**Table 1: Photocatalytic dye degradation**

Photocatalyst	Light Source	Application	Photocatalytic efficiency	Role of Cu	Reference
CuO	Visible light (tungsten-halogen-lamp(24 V/150 W) with a ranging between 380–800 nm)	Photo-degradation of MB, AY	43.5% degradation for MB and 66.3% for AY	Electrostatic interaction between dye and CuO	46
Cu <sub>2</sub> O	Visible light (100 W electric-bulb)	Photo-degradation of CR	0.0510 min <sup>-1</sup> rate constant using hollow octahedron	p-type semiconductor	51
Cu <sub>2</sub> O-Cu	Xe-lamp (100 W)	Photo-degradation of MO	-----	LSPR of metallic Cu	57
Cu <sub>2</sub> O covered by Cu nanoparticles	90 W W-lamp as visible-light source	Photo-degradation of MB	88% photo-degradation was achieved	LSPR of Cu	60
Cu film/Cu <sub>2</sub> O/TiO <sub>2</sub>	450W Xe-lamp	Photo-degradation of MB	98% photo-degradation was achieved	efficient charge separation and SPR	62
Cu/Cu <sub>2</sub> O/ZnO	100 W bulb as visible-lightsource	Photo-degradation of MB	Rate constant was 0.0185 min <sup>-1</sup>	n-p hetero-junction, Schottky barrier, LSPR	63
Copper oxide-titanate nanobelt and copper-titanate nanobelt	150 W Xe-lamp (400 nm UV cut-off filter)	Photo-degradation of MO	-----	interfacial electron-charge transfer and LSPR	64
Cu/ BaTiO <sub>3</sub>	UV-Vis light with a 500 W Xe-lamp	Photo-degradation of RhB	42% degradation was achieved	inter-band transition associated SPR effect	66
Cu/TiO <sub>2</sub>	300 W high pressure lamp	Photo-degradation of MB	70% degradation was achieved	synergistic effect of Schottky barrier and SPR	67
Cu particles <i>In-situ</i> loaded on TiO <sub>2</sub> surface	300 W Xe-lamp	Reductive debromination of decabrominated diphenyl ether	-----	SPR	68
Cu@CuNi/ZnO	UV light	Photo-degradation of RhB	-----	increased life-time of photo-produced electrons and holes	70
CuO/Cu <sub>2</sub> O	300W Xe-lamp as visible light source	Photo-degradation of MB	-----	Hetero-junction increases the charge collection, and decreases the recombination of e-/h+ pair	71
Cu/Cu <sub>2</sub> O/CuO nanocomposites	125 W high vapor pressure Hg lamp as UV light source	Photo-degradation of CR and MG	80% and 60% degradation were achieved for CR and MG, respectively	oxygen vacancy in the material and hetero-junction pattern	72

**Table 2: Photocatalytic generation of H<sub>2</sub>**

Photocatalyst	Dosages of Catalyst	Light Source	Sacrificial agent	H <sub>2</sub> yield	Role of Cu	Reference
Cu/TiO <sub>2</sub>	10 mg	Simulated-light ( $\lambda \geq 700$ nm)	CH <sub>3</sub> OH	8.12 mmol•h <sup>-1</sup> •g <sup>-1</sup>	LSPR-induced photothermal effect	81
Cu/TiO <sub>2</sub>	1 g/L	Light of various spectral ranges ( $\geq 420$ nm or $\geq 500$ nm)	CH <sub>3</sub> OH	30% increase in H <sub>2</sub> evaluation	SPR effect	84
Cu/TiO <sub>2</sub>	4.0 cm <sup>2</sup>	Xe-lamp of $\lambda > 400$ nm	Ethelene glycol	3.0 $\mu\text{mol} (\text{hcm}^2)^{-1}$	SPR effect	85
Cu decorated TiO <sub>2</sub>	0.4 g/L	White-light (500 W Xe lamp)	CH <sub>3</sub> OH	383 $\mu\text{mol g}^{-1} \text{h}^{-1}$	SPR effect	86
Cu/CuFe <sub>2</sub> O <sub>4</sub>	-----	light	Not used	2.26 mmol g <sup>-1</sup> h <sup>-1</sup> ,	LSPR effect	87
Cu@Cu <sub>2</sub> O/ZnO	-----	UV-Vis light	Na <sub>2</sub> S and Na <sub>2</sub> SO <sub>3</sub>	1472.2 $\mu\text{mol h}^{-1} \text{g}^{-1}$	LSPR effect	88
Cu-SrTiO <sub>3</sub>	0.2 g	300 W Xe arc lamp of $\lambda > 400$ nm	CH <sub>3</sub> OH	76.3 $\mu\text{mol h}^{-1} \text{g}^{-1}$	mitigates Fano interference and LSPR effect	89
CuCo bimetal	5 mg	Sun-light	Not used	77.1 $\mu\text{mol h}^{-1} \text{g}^{-1}$	SPR effect	90
CuCo bimetal/rGO	5 mg	300 W Xe-lamp which stimulates sun-light	Not used	365.7 $\mu\text{mol h}^{-1} \text{g}^{-1}$	Landau damping and SPR	93
CuNi/rGO	5 mg	300 W Xe-lamp for simulated sun-light source	Lactic acid	1787 $\mu\text{mol h}^{-1} \text{g}^{-1}$	LSPR	94
Cu/WS <sub>2</sub>	3 mg	Simulate sun-light that includes NIR	Lactic acid	64 mmol h <sup>-1</sup> g <sup>-1</sup>	SPR effect, Schottkyinterface	95

**Table 3: Photocatalytic CO<sub>2</sub>RR**

Photocatalyst	Catalyst dosage	Light Source	Reaction system	Product	Role of Cu	Reference
Cu-loaded TiO <sub>2</sub>	50 mg	300 W simulated solar Xe arc lamp	NaHCO <sub>3</sub> (0.1 g) and 0.3 mL of 2 M H <sub>2</sub> SO <sub>4</sub>	CH <sub>4</sub> : 8.04 μmol g <sup>-1</sup> h <sup>-1</sup>	Increases light absorption, electron trap	101
Cu@TiO <sub>2</sub>	-----	Xe-lamp (300 W)	-----	CO: 32.5 μmol g <sup>-1</sup> h <sup>-1</sup>	Active centre	102
Cu@TiO <sub>2</sub>	10 mg	Xe-lamp (300 W)	100 mL water, high purity CO <sub>2</sub> was bubbled	CO: activity of Cu/TiO <sub>2</sub> is 10 times than TiO <sub>2</sub>	Fast electron transfer	103
Cu/m-TiO <sub>2</sub>	20 mg	300W Xe arc lamp	CO <sub>2</sub> +H <sub>2</sub> O	CH <sub>4</sub> : 8 times greater than bare TiO <sub>2</sub>	Fast electron transfer	104
Cu/ TiO <sub>2</sub>	-----	16 W high-pressure Hg-lamp and 500 W Xe-lamp (420 nm cut-off)	CO <sub>2</sub> +H <sub>2</sub> O	MeOH: 1.8 mmol cm <sup>-2</sup> h <sup>-1</sup>	Charge transfer property and LSPR effect	105
Cu/Co core/shell bimetal	10 mg	Xe-lamp (300 W)	4 mL H <sub>2</sub> O, 2 mL lactic acid	CO: 11043.33 μmol g <sup>-1</sup>	Rapid interfacial charge-transfer	107
Cu/CeO <sub>2</sub> -x	50 mg	Xe-lamp (300 W)	CO <sub>2</sub>	CO: 8.25 μmol g <sup>-1</sup>	Oxygen vacancy, active centres, increased light absorption	108
Cu/Bi <sub>4</sub> O <sub>5</sub> I <sub>2</sub>	-----	300 W Xe-lamp	-----	CO production rate of 7.34 μmol g <sup>-1</sup> h <sup>-1</sup>	Schottky junction, SPR effect	109
Cu/CsCuCl <sub>3</sub>	5 mg	150 W xe-lamp	4 mL of Ethyl acetate, and 1 mL of isopropyl alcohol	CH <sub>4</sub> ;selectivity up to 92.7%,	Charge separation	110

**CONCLUSION**

In conclusion, a plethora of research articles on photocatalysis using Cu in various nanomaterials are thoroughly summarized in the review. These kinds of photocatalysis have fetched noteworthy attention in scientific community owing to its low-cost, attractive LSPR effect, capability to construct Schottky junction and amazing activity. With potential applications to mitigate environmental crisis exploiting solar energy directly, these kinds of materials in

photocatalysis will be of huge interest in the near future.

**ACKNOWLEDGMENT**

This research did not receive any specific grant from funding agencies in the public, commercial, or not-for-profit sectors.

**Conflict of interest**

The author declare that we have no conflict of interest.

**REFERENCES**

1. Wu, N. Q.; Wang, J.; Tafen, D.; Wang, H.; Zheng, J. G.; Lewis, J. P.; Liu, X.; Leonard, S. S.; Manivannan, A. Shape-Enhanced Photocatalytic Activity of Single-Crystalline Anatase TiO<sub>2</sub> (101) Nanobelts., *J. Am. Chem. Soc.*, **2010**, *132*(19), 6679-6685.
2. Manthiram, K.; Alivisatos, A. P. Tunable Localized Surface Plasmon Resonances in Tungsten Oxide Nanocrystals., *J. Am. Chem. Soc.*, **2012**, *134*(9), 3995-3998.
3. Takeda, H.; Ohashi, K.; Sekine, A.; Ishitani, O. Photocatalytic CO<sub>2</sub> Reduction Using Cu(I) Photosensitizers with a Fe(II) Catalyst., *J. Am. Chem. Soc.*, **2016**, *138*(13), 4354-4357.
4. Sharma, V.; Kumar, S.; Krishnan, V. Clustered Au on TiO<sub>2</sub> Snowman Like Nanoassemblies for Photocatalytic Applications., *Chemistry Select.*, **2016**, *1*(11), 2963-2970.
5. Jiang, R.; Li, B.; Fang, C.; Wang, J. Metal/Semiconductor Hybrid Nanostructures for Plasmon-Enhanced Applications., *Adv. Mater.*, **2014**, *26*(31), 5274-5309.
6. Fang, C. H.; Jia, H. L.; Chang, S.; Ruan, Q. F.; Wang, P.; Chen, T.; Wang, J. F. (Gold core)/(titania shell) nanostructures for plasmon-enhanced photon harvesting and generation of reactive oxygen species., *Energy Environ. Sci.*, **2014**, *7*(10), 3431-3438.

7. Kuo, C. H.; Yang, Y. C.; Gwo, S.; Huang, M. H. Facet-Dependent and Au Nanocrystal-Enhanced Electrical and Photocatalytic Properties of Au–Cu<sub>2</sub>O Core–Shell Heterostructures., *J. Am. Chem. Soc.*, **2011**, *133*(4), 1052-1057.
8. Han, P.; Tana, T.; Xiao, Q.; Sarina, S.; Waclawik, E. R.; Gómez, D. E.; Zhu, H. Promoting Ni(II) Catalysis with Plasmonic Antennas., *Chem.*, **2019**, *5*(11), 2879-2889.
9. Chikkaraddy, R.; Nijs, B. D.; Benz, F.; Barrow, S. J.; Scherman, O. A.; Rosta, E.; Demetriadou, A.; Fox, P.; Hess, O.; Baumberg, J. J. Single-molecule strong coupling at room temperature in plasmonic nanocavities. *Nature.*, **2016**, *535*(7610), 127-130.
10. Reddy, H.; Wang, K.; Kudyshev, Z.; Zhu, L.; Yan, S.; Vezzoli, A.; Higgins, S. J.; Gavini, V.; Boltasseva, A.; Reddy, P.; Shalaev, V. M.; Meyhofer, E. Determining plasmonic hot-carrier energy distributions via single-molecule transport measurements., *Science.*, **2020**, *369*(6502), 423-426.
11. Wang, D.; Astruc, D. The recent development of efficient Earth-abundant transition-metal nanocatalysts., *Chem. Soc. Rev.*, **2017**, *46*(3), 816-854.
12. Lu, B.; Liu, A.; Wu, H.; Shen, Q.; Zhao, T.; Wang, J. Hollow Au-Cu<sub>2</sub>O core-shell nanoparticles with geometry-dependent optical properties as efficient plasmonic photocatalysts under visible light., *Langmuir.*, **2016**, *32*(12), 3085–3094.
13. Li, J.; Cushing, S. K.; Bright, J.; Meng, F.; Senty, T. R.; Zheng, P.; Bristow, A. D.; Wu, N. Ag@Cu<sub>2</sub>O Core-Shell Nanoparticles as Visible-Light Plasmonic Photocatalysts. *ACS Catal.*, **2013**, *3*(1), 47–51.
14. Zhan, C.; Moskovits, M.; Tian, Z.-Q. Recent Progress and Prospects in Plasmon-Mediated Chemical Reaction., *Matter.*, **2020**, *3*(1), 42-56.
15. Linic, S.; Christopher, P.; Ingram, D. B. Plasmonic-metal nanostructures for efficient conversion of solar to chemical energy., *Nat. Mater.*, **2011**, *10*(12), 911-921.
16. Linic, S.; Aslam, U.; Boerigter, C.; Morabito, M. Photochemical transformations on plasmonic metal nanoparticles., *Nat. Mater.*, **2015**, *14*(6), 567-576.
17. Kim, S.; Kim, J. M.; Park, J. E.; Nam, J. M. Nonnoble-Metal-Based Plasmonic Nanomaterials: Recent Advances and Future Perspectives., *Adv. Mater.*, **2018**, *30*(42), 1704528.
18. Yi, S.-S.; Zhang, X.-B.; Wulan, B.-R.; Yan, J.-M.; Jiang, Q. Non-noble metals applied to solar water splitting., *Energy Environ. Sci.*, **2018**, *11*, 3128-3156.
19. Gawande, M. B.; Goswami, A.; Felpin, F. X.; Asefa, T.; Huang, X.; Silva, R.; Zou, X.; Zboril, R.; Varma, R. S. Cu and Cu-Based Nanoparticles: Synthesis and Applications in Catalysis., *Chem. Rev.*, **2016**, *116*(6), 3722-3811.
20. Xin, Y.; Yu, K.; Zhang, L.; Yang, Y.; Yuan, H.; Li, H.; Wang, L.; Zeng, J. Copper-Based Plasmonic Catalysis: Recent Advances and Future Perspectives., *Adv. Mater.*, **2021**, *33*(32), 2008145.
21. Amirjani, A.; Amlashi, N. B.; and Ahmadiani, Z. S. Plasmon-Enhanced Photocatalysis Based on Plasmonic Nanoparticles for Energy and Environmental Solutions: A Review., *ACS Appl. Nano Mater.*, **2023**, *6*(11), 9085–9123.
22. An, K.; Hu, J.; Wang, J. Schottky-barrier-free plasmonic photocatalysts. *Phys. Chem., Chem. Phys.*, **2023**, *25*(19), 19358–19370.
23. Kreibig, U.; Vollmer, M. *Optical Properties of Metal Clusters*; Springer: Berlin, Germany., **1995**.
24. Chou, L.-W.; Shin, N.; Sivaram, S. V.; Filler, M. A. Tunable Mid-Infrared Localized Surface Plasmon Resonances in Silicon Nanowires., *J. Am. Chem. Soc.*, **2012**, *134*(39), 16155–16158.
25. Christopher, P.; Xin, H.; Marimuthu, A.; Linic, S., Singular Characteristics and Unique Chemical Bond Activation Mechanisms of Photocatalytic Reactions on Plasmonic Nanostructures., *Nature Materials.*, **2012**, *11*(12), 1044-1050.
26. Duan, S.; Ai, Y.-J.; Hu, W.; Luo, Y., Roles of Plasmonic Excitation and Protonation on Photoreactions of P-Aminobenzenethiol on Ag Nanoparticles., *J. Phys. Chem. C.*, **2014**, *118*(13), 6893-6902.
27. Kale, M. J.; Avanesian, T.; Christopher, P.; Direct Photocatalysis by Plasmonic Nanostructures., *ACS Catalysis.*, **2014**, *4*(1), 116-128.
28. Gomes Silva, C.; Juarez, R.; Marino, T.; Molinari, R.; Garcia, H., Influence of Excitation Wavelength (UV or Visible Light) on the Photocatalytic Activity of Titania Containing Gold Nanoparticles for the Generation of Hydrogen or Oxygen from Water., *J. Am. Chem. Soc.*, **2010**, *133*(3), 595-602.

29. Seh, Z. W.; Liu, S.; Low, M.; Zhang, S. Y.; Liu, Z.; Mlayah, A.; Han, M. Y., Janus Au-TiO<sub>2</sub> Photocatalysts with Strong Localization of Plasmonic near-Fields for Efficient Visible-Light Hydrogen Generation., *Adv. Mater.*, **2012**, *24*(17), 2310-2314.
30. Mukherjee, S.; Libisch, F.; Large, N.; Neumann, O.; Brown, L. V.; Cheng, J.; Lassiter, J. B.; Carter, E. A.; Nordlander, P.; Halas, N. J., Hot Electrons Do the Impossible: Plasmon-Induced Dissociation of H<sub>2</sub> on Au., *Nano Lett.*, **2013**, *13*(1), 240-247.
31. Hou, W.; Hung, W. H.; Pavaskar, P.; Goepfert, A.; Aykol, M.; Cronin, S. B., Photocatalytic Conversion of CO<sub>2</sub> to Hydrocarbon Fuels Via Plasmon-Enhanced Absorption and Metallic Interband Transitions., *ACS Catalysis.*, **2011**, *1*(8), 929-936.
32. Gelle, A.; Jin, T.; de la Garza, L.; Price, G. D.; Besteiro, L. V.; Moores, A. Applications of Plasmon-Enhanced Nanocatalysis to Organic Transformations., *Chem. Rev.*, **2020**, *120*(2), 986-1041.
33. Han, P.; Tana, T.; Xiao, Q.; Sarina, S.; Waclawik, E. R.; Gómez, D. E.; Zhu, H. Promoting Ni(II) Catalysis with Plasmonic Antennas., *Chem.*, **2019**, *5*(11), 2879-2899.
34. Liu, Z.; Zhong, Y.; Shafei, I.; Jeong, S.; Wang, L.; Nguyen, H. T.; Sun, C.-J.; Li, T.; Chen, J.; Chen, L.; Losovyj, Y.; Gao, X.; Ma, W.; Ye, X. Broadband Tunable Mid-Infrared Plasmon Resonances in Cadmium Oxide Nanocrystals Induced by Size-Dependent Nonstoichiometry., *Nano Lett.*, **2020**, *20*(4), 2821-2828.
35. Sambou, A.; Ngom, B. D.; Gomis, L.; Beye, A. C. Turnability of the Plasmonic Response of the Gold Nanoparticles in Infrared Region., *American Journal of Nanomaterials.*, **2016**, *4*(3), 63-69.
36. Li, S.; Miao, P.; Zhang, Y.; Wu, J.; Zhang, B.; Du, Y.; Han, X.; Sun, J.; Xu, P. Recent Advances in Plasmonic Nanostructures for Enhanced Photocatalysis and Electrocatalysis., *Adv. Mater.*, **2020**, *33*(6), 2000086.
37. Brongersma, M. L.; Halas, N. J.; Nordlander, P. Plasmon-induced hot carrier science and technology., *Nat. Nanotechnol.*, **2015**, *10*(1), 25-34.
38. Alejro, M.; Jun, G. L.; Vikram, K.; Peter, N. Plasmon-induced hot carriers in metallic nanoparticles., *ACS Nano.*, **2014**, *8*(8), 7630-8.
39. Hartland, G. V.; Besteiro, L. V.; Johns, P.; Govorov, A. O. What's so Hot about Electrons in Metal Nanoparticles? *ACS Energy Lett.*, **2017**, *2*(7), 1641-1653.
40. Gawande, M. B.; Goswami, A.; Felpin, F.-X.; Asefa, T.; Huang, X.; Silva, R.; Zou, X.; Zboril, R.; Varma, R. S. Cu and Cu-Based Nanoparticles: Synthesis and Applications in Review Catalysis., *Chem. Rev.*, **2016**, *116*(6), 3722-3811.
41. Yang, X.; Li, Q.; Li, L.; Lin, J.; Yang, X.; Yu, C.; Liu, Z.; Fang, Y.; Huang, Y.; Tang, C. CuCo binary metal nanoparticles supported on boron nitride nanofibers as highly efficient catalysts for hydrogen generation from hydrolysis of ammonia borane., *J. Power Sources.*, **2019**, *431*, 135-143.
42. Bian, Z.; Tachikawa, T.; Zhang, P.; Fujitsuka, M.; Majima, T. Au/TiO<sub>2</sub> superstructure-based plasmonic photocatalysts exhibiting efficient charge separation and unprecedented activity., *J. Am. Chem. Soc.*, **2014**, *136*(1), 458-465.
43. Stewart, S.; Wei, Q.; Sun, Y. Surface chemistry of quantum-sized metal nanoparticles under light illumination., *Chem. Sci.*, **2021**, *12*(4), 1227-1239.
44. Li, M.; Cushing, S. K.; Wang, Q.; Shi, X.; Hornak, L. A.; Hong, Z.; Wu, N. Size-Dependent Energy Transfer between CdSe/ZnS Quantum Dots and Gold Nanoparticles., *J. Phys. Chem. Lett.*, **2011**, *2*(17), 2125-2129.
45. Sibhatu, A. K.; Weldegebrieal, G. K.; Sagadevan, S.; Tran, N. N.; Hessel, V. Photocatalytic activity of CuO nanoparticles for organic and inorganic pollutants removal in wastewater remediation., *Chemosphere.*, **2022**, *300*, 134623 (1-18).
46. Ramesh, M. CuO as efficient photo catalyst for photocatalytic decoloration of wastewater containing Azo dyes., *Water Practice & Technology.*, **2021**, *16*(4), 1078-1090.
47. Raghav, R.; Aggarwal, P.; Srivastava, S. Tailoring oxides of copper-Cu<sub>2</sub>O and CuO nanoparticles and evaluation of organic dyes degradation. In: AIP Conference Proceedings, **2016**, 1724. AIP Publishing, p. 020078.



48. Katwal, R.; Kaur, H.; Sharma, G.; Naushad, M.; Pathania, D. Electrochemical synthesized copper oxide nanoparticles for enhanced photocatalytic and antimicrobial activity., *Journal of Industrial and Engineering.*, **2015**, *31*, 173–184.
49. Su, Q.; Zuo, C.; Liu, M.; Tai, X. A Review on Cu<sub>2</sub>O-Based Composites in Photocatalysis: Synthesis, Modification, and Applications. *Molecules.*, **2023**, *28*(14), 5576 (1-25).
50. Yu, Y.; Huang, W. Y.; Du, F. P.; Ma, L. L. Synthesis and Characteristic of Cuprous Oxide Nano-Whiskers with Photocatalytic Activity under Visible Light., *Materials Science Forum.*, **2005**, *475–479*, 3531–3534.
51. Pal, J.; Ganguly, M.; Mondal, C.; Roy, A.; Negishi, Y.; Pal, T. Crystal-Plane-Dependent Etching of Cuprous Oxide Nanoparticles of Varied Shapes and Their Application in Visible Light Photocatalysis., *J. Phys. Chem. C.*, **2013**, *117*(46), 24640–24653.
52. Zuo, S.; Xu, H.; Liao, W.; Yuan, X.; Sun, L.; Li, Q.; Zan, J.; Li, D.; Xia, D. Molten-salt synthesis of g-C<sub>3</sub>N<sub>4</sub>-Cu<sub>2</sub>O heterojunctions with highly enhanced photocatalytic performance., *Colloids Surf. A.*, **2018**, *546*, 307–315.
53. Yue, Y.; Zhang, P.; Wang, W.; Cai, Y.; Tan, F.; Wang, X.; Qiao, X.; Wong, P. K. Enhanced dark adsorption and visible-light-driven photocatalytic properties of narrower-band-gap Cu<sub>2</sub>S decorated Cu<sub>2</sub>O nanocomposites for efficient removal of organic pollutants., *J. Hazard. Mater.*, **2020**, *384*, 121302.
54. Cheng, L.; Tian, Y.; Zhang, J. Construction of p-n heterojunction film of Cu<sub>2</sub>O/Fe<sub>2</sub>O<sub>3</sub> for efficiently photoelectrocatalytic degradation of oxytetracycline., *J. Colloid Interface Sci.*, **2018**, *526*, 470–479.
55. Li, Z.; Liu, D.; Huang, W.; Sun, Y.; Li, S.; Wei, X.; Applying facilely synthesized CuO/CeO<sub>2</sub> photocatalyst to accelerate methylene blue degradation in hypersaline wastewater., *J. Surf. Interface Anal.*, **2019**, *51*(3), 336-344.
56. Ma, P.; Yu, Y.; Xie, J.; Fu, Z. Ag<sub>3</sub>PO<sub>4</sub>/CuO composites utilizing the synergistic effect of photocatalysis and Fenton-like catalysis to dispose organic pollutants. *Adv. Powder Technol.*, **2017**, *28*(11), 2797-2804.
57. Sugawa, K.; Tsunenari, N.; Takeda, H.; Fujiwara, S.; Akiyama, T.; Honda, J.; Igari, S.; Tokuda, K.; Takeshima, N.; Watanuki, Y.; Tsukahara, S.; Takase, K.; Umegaki, T.; Kojima, Y.; Nishimiya, N.; Fukuda, N.; Kusaka, Y.; Ushijima, H.; Otsuki, J. Development of Plasmonic Cu<sub>2</sub>O/Cu Composite Arrays as Visible- and Near- Infrared-Light-Driven Plasmonic Photocatalysts., *Langmuir.*, **2017**, *33*(23), 5685–5695.
58. Cushing, S. K.; Li, J.; Meng, F.; Senty, T. R.; Suri, S.; Zhi, M.; Li, M.; Bristow, A. D.; Wu, N. Photocatalytic Activity Enhanced by Plasmonic Resonant Energy Transfer from Metal to Semiconductor., *J. Am. Chem. Soc.*, **2012**, *134*(36), 15033–15041.
59. Siripala, W.; Ivanovskaya, A.; Jaramillo, T. F.; Baeck, S.-H.; McFarland, E. W. A Cu<sub>2</sub>O/TiO<sub>2</sub> Heterojunction Thin Film Cathode for Photoelectrocatalysis., *Sol. Energy Mater. Sol. Cells.*, **2003**, *77*(3), 229-237.
60. Cheng, Y.; Lin, Y.; Xu, J.; He, J.; Wang, T.; Yu, G.; Shao, D.; Wang, W.; Lu, F.; Li, L.; Du, X.; Wang, W.; Liu, H.; Zheng, R. Surface plasmon resonance enhanced visible-light-driven photocatalytic activity in Cu nanoparticles covered Cu<sub>2</sub>O microspheres for degrading organic pollutants., *Appl. Surf. Sci.*, **2016**, *366*, 120–128.
61. Lu, W.W.; Gao, S.Y.; Wang, J. J. One-pot synthesis of Ag/ZnO self-assembled 3D hollow microspheres with enhanced photocatalytic performance., *J. Phys. Chem C.*, **2008**, *112*(43) 16792–16800.
62. Rekeb, L.; Hamadou, L.; Kadri, A.; Benbrahim, N.; Chainet, E. Highly broadband plasmonic Cu film modified Cu<sub>2</sub>O/TiO<sub>2</sub> nanotube arrays for efficient photocatalytic performance., *International Journal of Hydrogen Energy.*, **2019**, *44*(21) 10541-10553.
63. Pal, J.; Sasmal, A. K.; Ganguly, M.; Pal, T. Surface Plasmon Effect of Cu and Presence of n-p Hetero- Junction in Oxide Nanocomposites for Visible Light Photocatalysis., *J. Phys. Chem. C.*, **2015**, *119*(7) , 3780–3790.
64. Logar, M.; Bracko, I.; Potocnik, A.; Jancar, B. Cu and CuO/Titanate Nanobelt Based Network Assemblies for Enhanced Visible Light Photocatalysis., *Langmuir.*, **2014**, *30*(16), 4852–4862.
65. Linic, S.; Christopher, P.; Ingram, D. B. Plasmonic–Metal Nanostructures for Efficient Conversion of Solar to Chemical Energy., *Nat. Mater.*, **2011**, *10*(12), 911–921.

66. Zhang, S.; Li, S.; Zhang, B.; Yu, D.; Zhang, Z.; Li, J. Copper-nanoparticle-dispersed amorphous BaTiO<sub>3</sub> thin films as hole-trapping centers: enhanced photocatalytic activity and stability., *RSC Adv.*, **2019**, *9*(9), 5045-5052.
67. Dong, J.; Ye, J.; Ariyanti, D.; Wang, Y.; Wei, S.; Gao, W. Enhancing photocatalytic activities of titanium dioxide via well-dispersed copper nanoparticles., *Chemosphere.*, **2018**, *204* (10), 193-201.
68. Lv, Y.; Cao, X.; Jiang, H.; Song, W.; Chen, C.; Zhao, J. Rapid photocatalytic debromination on TiO<sub>2</sub> with in-situ formed copper co-catalyst: Enhanced adsorption and visible light activity., *Applied Catalysis B: Environmental.*, **2016**, *194*, 150–156.
69. Yang, X.; Zhong, H.; Zhu, Y.; Jiang, H.; Shen, J.; Huang, J.; Li, C. Highly efficient reusable catalyst based on silicon nanowire arrays decorated with copper nanoparticles., *J. Mater. Chem. A.*, **2014**, *2*(24), 9040-9047.
70. Zeng, D.; Gong, P.; Chen, Y.; Zhang, Q.; Xie, Q.; Peng, D. Colloidal Synthesis of Cu-ZnO and Cu@CuNi-ZnO Hybrid Nanocrystals with Controlled Morphologies and Multifunctional Properties., *Nanoscale.*, **2016**, *8*(2), 11602-11610.
71. Khiavi, N. D.; Katal, R.; Eshkalak, S. K.; Masudy-Panah, S.; Ramakrishna, S.; Jiangyong, H. Visible Light Driven Heterojunction Photocatalyst of CuO–Cu<sub>2</sub>O Thin Films for Photocatalytic Degradation of Organic Pollutants., *Nanomaterials.*, **2019**, *9* (7), 1011 (1-12).
72. Kumar, S.; Bhawna, Gupta, A.; Kumar, R.; Bharti, A.; Kumar, A.; Kumar, V. New Insights into Cu/Cu<sub>2</sub>O/CuO Nanocomposite Heterojunction Facilitating Photocatalytic Generation of Green Fuel and Detoxification of Organic Pollutants., *J. Phys. Chem. C.*, **2023**, *127*(15), 7095–7106.
73. Zhou, H.; Fan, T.; Zhang, D. An insight into artificial leaves for sustainable energy inspired by natural photosynthesis., *Chem Cat Chem.*, **2011**, *3*(3), 513-528.
74. Tu, W.; Zhou, Y.; Zou, Z.; Photocatalytic conversion of CO<sub>2</sub> into renewable hydrocarbon fuels: state-of-the-art accomplishment, challenges, and prospects., *Adv Mater.*, **2014**, *26*(27), 4607-4626.
75. Chen, S.; Takata, T.; Domen, K. Particulate photocatalysts for overall water splitting., *Nat. Rev. Mater.*, **2017**, *2*(10), 17050 (1-16).
76. Chen, L. H.; Chen, R.; Hu, H. F.; Li, G. H. Enhancement of photocatalytic hydrogen production of semiconductor by plasmonic silver nanocubes under visible light., *Mater. Lett.*, **2019**, *242*, 47–50.
77. Kudo, A.; Miseki, Y. Heterogeneous photocatalyst materials for water splitting., *Chem. Soc. Rev.*, **2009**, *38*(1), 253–278.
78. Wang, W.; Xu, M. G.; Xu, X. M.; Zhou, W.; Shao, Z. P. Perovskite oxide based electrodes for high-performance photoelectrochemical water splitting. *Angew., Chem., Int. Ed.*, **2020**, *59*(1), 136–152.
79. Yi, S.-S.; Zhang, X.-B.; Wulan, B.-R.; Yan, J.-M.; Jiang, Q. Non-noble metals applied to solar water splitting., *Energy Environ. Sci.*, **2018**, *11*(11), 3128 -3156.
80. Wang, Z.; Li, C.; Domen, K. Recent developments in heterogeneous photocatalysts for solar-driven overall water splitting., *Chem. Soc. Rev.*, **2019**, *48*(7), 2109-2125.
81. Song, R.; Liu, M.; Luo, B.; Geng, J.; Jing, D. Plasmon-induced Photothermal Effect of Sub-10-nm Cu Nanoparticles Enables Boosted Full-spectrum Solar H<sub>2</sub> Production., *Reaction Engineering, Kinetics and Catalysis.*, **2020**, *66*(11), e1708.
82. Tembhurne, S.; Nandjou, F.; Haussener, S. A thermally synergistic photo-electrochemical hydrogen generator operating under concentrated solar irradiation., *Nat Energy.*, **2019**, *4*(5), 399.
83. Nishijima, Y.; Ueno, K.; Kotake, Y.; Murakoshi, K.; Inoue, H.; Misawa, H. Near-Infrared Plasmon-Assisted Water Oxidation., *J Phys Chem Lett.*, **2012**, *3*(10), 1248-1252.
84. Nie, J.; Patrocínio, A. O. T.; Hamid, S.; Sieland, F.; Sann, J.; Xia, S.; Bahnmann, D. W.; Schneider, J. New Insights into the Plasmonic Enhancement for Photocatalytic H<sub>2</sub> Production by Cu-TiO<sub>2</sub> upon Visible Light Illumination., *Phys. Chem. Chem. Phys.*, **2018**, *20*(7), 5264-5273.
85. Zhang, S.; Peng, B.; Yang, S.; Wang, H.; Yu, H.; Fang, Y.; Peng, F. Non-noble metal copper nanoparticles-decorated TiO<sub>2</sub> nanotube arrays with plasmon-enhanced photocatalytic hydrogen evolution under visible light., *International Journal of Hydrogen Energy.*, **2015**, *40*(1), 303-310.

86. Liu, P.; Dorfler, A.; Tabrizi, A. A.; Skokan, L.; Rawach, D.; Wang, P.; Peng, Z.; Zhang, J.; Ruediger, A. P.; Claverie, J. P. In Operando Photoswitching of Cu Oxidation States in Cu-Based Plasmonic Heterogeneous Photocatalysis for Efficient H<sub>2</sub> Evolution *ACS Appl. Mater. Interfaces.*, **2023**, *15*(23), 27832–27844.
87. Wang, A.; Yang, H.; Song, T.; Sun, Q.; Liu, H.; Wang, T.; Zeng, H. Plasmon mediated Fe-O in octahedral site of cuprospinel by Cu NPs for photocatalytic hydrogen evolution., *Nanoscale.*, **2017**, *9*(41), 15760-15765.
88. Lou, Y.; Zhang, Y.; Cheng, L.; Chen, J.; Zhao, Y. A Stable Plasmonic Cu@Cu<sub>2</sub>O/ZnO Heterojunction for Enhanced Photocatalytic H<sub>2</sub> Generation., *Chem Sus Chem.*, **2018**, *11*(9), 1505-1511.
89. Zhang, X.; Fu, A.; Chen, X.; Liu, L.; Ren, L.; Tong, L.; Ye, J. Highly Efficient Cu Induced Photocatalysis for Visible-light Hydrogen Evolution., *Catalysis Today.*, **2019**, *335*(1), 166-172.
90. Zhang, P.; Zeng, G.; Song, T.; Huang, S.; Wang, T.; Zeng, H. Design of plasmonic CuCo bimetal as a nonsemiconductor photocatalyst for synchronized hydrogen evolution and storage., *Applied Catalysis B: Environmental.*, **2019**, *242*, 389-396.
91. Li, J.; Cushing, S. K.; Meng, F.; Senty, T. R.; Bristow, A. D.; Wu, N. Plasmon-induced resonance energy transfer for solar energy conversion., *Nature Photonics.*, **2015**, *9*, 601-607.
92. Petek, H.; Ogawa, S. Femtosecond time-resolved two-photon photoemission studies of electron dynamics in metals., *Prog. Surf. Sci.*, **1997**, *56*(4), 239-310.
93. Zhang, P.; Liu, H.; Li, X. Plasmon-driven engineering in bimetallic CuCo combined with reduced graphene oxide for photocatalytic overall water splitting., *Appl. Surf. Sci.*, **2021**, *559* (1) 149865.
94. Zhang, P.; Song, T.; Wang, T.; Zeng, H. Fabrication of a non-semiconductor photocatalytic system using dendrite-like plasmonic CuNi bimetal combined with a reduced graphene oxide nanosheet for near-infrared photocatalytic H<sub>2</sub> evolution., *J. Mater. Chem. A.*, **2017**, *5*(43), 22772-22781.
95. Xu, X.; Luo, F.; Tang, W.; Hu, J.; Zeng, H.; Zhou, Y. Enriching Hot Electrons via NIR-Photon-Excited Plasmon in WS<sub>2</sub>@Cu Hybrids for Full-Spectrum Solar Hydrogen Evolution., *Adv. Funct. Mater.*, **2018**, *28*(43), 1804055.
96. Zhang, J.; Guan, B.; Wu, X.; Chen, Y.; Guo, J.; Ma, Z.; Bao, S.; Jiang, X.; Chen, L.; Shu, K.; Dang, H.; Guo, Z.; Li, Z.; Huang, Z. Research on photocatalytic CO<sub>2</sub> conversion to renewable synthetic fuels based on localized surface plasmon resonance: current progress and future perspectives., *Catal. Sci. Technol.*, **2023**, *13*(7), 1932–1975.
97. Ezendam, S.; Herran, M.; Nan, L.; Gruber, C.; Kang, Y.; Grobmeyer, F.; Lin, R.; Gargiulo, J.; Sousa-Castillo, A.; Cortes, E. Hybrid Plasmonic Nanomaterials for Hydrogen Generation and Carbon Dioxide Reduction., *ACS Energy Lett.*, **2022**, *7*(2), 778–815.
98. Chen, S.; Hai, G.; Gao, H.; Chen, X.; Li, A.; Zhang, X.; Dong, W. Modulation of the charge transfer behavior of Ni(II)-doped NH<sub>2</sub>-MIL-125(Ti): Regulation of Ni ions content and enhanced photocatalytic CO<sub>2</sub> reduction performance., *Chem. Eng. J.*, **2021**, *406*, 126886–126895.
99. Song, C.; Liu, X.i.; Xu, M.; Masi, D.; Wang, Y.; Deng, Y.; Zhang, M.; Qin, X.; Feng, K.; Yan, J.; Leng, J.; Wang, Z.; Xu, Y.; Yan, B.; Jin, S.; Xu, D.; Yin, Z.; Xiao, D.; Ma, D. Photothermal conversion of CO<sub>2</sub> with tunable selectivity using Fe-based catalysts: from oxide to carbide., *ACS Catal.*, **2020**, *10*(18), 10364–10374.
100. N. Stephanie, B. Erlend, B. S. Soren, L. Xinyan, K. E. Albert, H. Sebastian, S. Brian, E. L. S. Ifan, C. Karen, H. Christopher, K. N. Jens, F. J. Thomas, C. Ib, Progress and Perspectives of Electrochemical CO<sub>2</sub> Reduction on Copper in Aqueous Electrolyte., *Chem. Rev.*, **2019**, *119*(12), 7610-7672.
101. Zhang, T., Low, J.; Huang, X.; Al-Sharab, J. F.; Yu, J.; Asefa T. Copper-Decorated Microsized Nanoporous TiO<sub>2</sub> Photocatalysts for CO<sub>2</sub> Reduction by H<sub>2</sub>O., *Chem Cat Chem.*, **2017**, *9*(15), 3054-3062.
102. Lan, Y.; Xie, Y.; Chen, J.; Hu, Z.; Cui, D. Selective photocatalytic CO<sub>2</sub> reduction on coppertitanium dioxide-a study of the relationship between CO production and H<sub>2</sub> suppression., *Chem. Commun.*, **2019**, *55* (56), 8068-8071.

103. Jiang, Z.; Sun, W.; Miao, W.; Yuan, Z.; Yang, G.; Kong, F.; Yan, T.; Chen, J.; Huang, B.; An, C.; Ozin, G. A. Living Atomically Dispersed Cu Ultrathin TiO<sub>2</sub> Nanosheet CO<sub>2</sub> Reduction Photocatalyst *Adv. Sci.*, **2019**, *6*(15), 1900289 (1-5).
104. Yuan, L.; Hung, S.; Tang, Z.; Chen, H.; Xiong, Y.; Xu, Y. Dynamic Evolution of Atomically Dispersed Cu Species for CO<sub>2</sub> Photoreduction to Solar Fuels., *ACS Catal.*, **2019**, *9*(6), 4824–4833.
105. Liu, E.; Qi, L.; Bian, J.; Chen, Y.; Hu, X.; Fan, J.; Liu, H.; Zhu, C.; Wang, Q. A facile strategy to fabricate plasmonic Cu modified TiO<sub>2</sub> nanoflower films for photocatalytic reduction of CO<sub>2</sub> to methanol., *Materials Research Bulletin.*, **2015**, *68*, 203–209.
106. Wang, Z.-j.; Song, H.; Pang, H.; Ning, Y.; Duy, D. T.; Wang, Z.; Chen, H.; Weng, Y.; Fu, Q.; Nagao, T.; Fang, Y.; Ye, J. Photo-assisted methanol synthesis via CO<sub>2</sub> reduction under ambient pressure over plasmonic Cu/ZnO catalysts., *Appl. Catal. B.*, **2019**, *250*, 10-16.
107. Lai, H.; Xiao, W.; Wang, Y.; Song, T.; Long, B.; Yin, S.; Ali, A.; Deng, G.-J. Plasmon-induced carrier separation boosts high-selective photocatalytic CO<sub>2</sub> reduction on dagger-axe-like Cu@Co core-shell bimetal., *Chemical Engineering Journal.*, **2021**, *417*, 129295.
108. Wang, M.; Shen, M.; Jin, X.; Tian, J.; Li, M.; Zhou, Y.; Zhang, L.; Li, Y.; Shi, J. Oxygen vacancy generation and stabilization in CeO<sub>2-x</sub> by Cointroduction with improved CO<sub>2</sub> photocatalytic reduction activity., *ACS Catal.*, **2019**, *9*(5), 4573-4581.
109. Huang, Q.; Lin, J.; Yang, D.; Hu, Y.; Zhou, G.; Li, W.; Hu, J.; Yang, Z. Synergism of the Plasmonic Effect and Schottky Junction to Effectively Facilitate Photocatalytic CO<sub>2</sub> Reduction of Bi<sub>4</sub>O<sub>5</sub>I<sub>2</sub>@Cu., *ACS Sustainable Chem. Eng.*, **2023**, *11*(48), 17168–17178.
110. Zhao, H.; Huang, J.; Qin, Q.; Chen, H.; Kuang, D. In Situ Loading of Cu Nanocrystals on CsCuCl<sub>3</sub> for Selective Photoreduction of CO<sub>2</sub> to CH<sub>4</sub>., *Small.*, **2023**, *19*(45), 2302022.
111. Christopher, P.; Xin, H.; Linic, S. Visible-light-enhanced catalytic oxidation reactions on plasmonic silver nanostructures., *Nat. Chem.*, **2011**, *3*(6), 467-472.
112. Huang, Y.; Liu, Z.; Gao, G.; Xiao, G.; Du, A.; Bottle, S.; Sarina, S.; Zhu, H. Stable Copper Nanoparticle Photocatalysts for Selective Epoxidation of Alkenes with Visible Light., *ACS Catal.*, **2017**, *7*(8), 4975–4985.
113. Gan, Y.; Zhang, M.; Xiong, J.; Zhu, J.; Li, W.; Zhang, C.; Cheng, G. Impact of Cu particles on adsorption and photocatalytic capability of mesoporous Cu@TiO<sub>2</sub> hybrid towards ciprofloxacin antibiotic removal., *J. Taiwan Inst. Chem. Eng.*, **2019**, *96*, 229.
114. Liu, Y.; Wu, Q.; Zhao, Y. Biomimetic synthesis of Ag<sub>3</sub>PO<sub>4</sub>-NPs/Cu-NWs with visible-light-enhanced photocatalytic activity for degradation of the antibiotic ciprofloxacin., *Dalton Trans.*, **2017**, *46*(19), 6425-6432.
115. Farooqi, Z. H.; Akram, M. W.; Begum, R.; Wu, W.; Irfan, A. Inorganic nanoparticles for reduction of hexavalent chromium: Physicochemical aspects., *J. Hazard. Mater.*, **2021**, *402*, 123535.
116. Patnaik, S.; Swain, G.; Parida, K. M. Highly efficient charge transfer through a double Z-scheme mechanism by a Cu-promoted MoO<sub>3</sub>/g-C<sub>3</sub>N<sub>4</sub> hybrid nanocomposite with superior electrochemical and photocatalytic performance., *Nanoscale.*, **2018**, *10*(13), 5950-5964.